

We are IntechOpen, the world's leading publisher of Open Access books Built by scientists, for scientists

6,900

Open access books available

186,000

International authors and editors

200M

Downloads

Our authors are among the

154

Countries delivered to

TOP 1%

most cited scientists

12.2%

Contributors from top 500 universities



WEB OF SCIENCE™

Selection of our books indexed in the Book Citation Index
in Web of Science™ Core Collection (BKCI)

Interested in publishing with us?
Contact book.department@intechopen.com

Numbers displayed above are based on latest data collected.
For more information visit www.intechopen.com



Volume Bragg Gratings: Fundamentals and Applications in Laser Beam Combining and Beam Phase Transformations

Ivan Divliansky

Additional information is available at the end of the chapter

<http://dx.doi.org/10.5772/66958>

Abstract

Two major volume Bragg grating (VBG) applications will be presented and in particular laser beam combining and holographically encoded phase masks. Laser beam combining is an approach where multiple lasers are combined to produce more power. Spectral beam combining is a technique in which different wavelengths are superimposed spatially (combined) using a dispersive element such as a volume Bragg grating. To reduce the complexity of such combining system instead of multiple individual VBGs, it will be demonstrated that a single holographic element with multiple VBGs recorded inside could be used for the same purpose. Similar multiplex volume holographic elements could be used for coherent beam combining. In this case, the gratings operate at the same wavelength and have degenerate output. Such coherent combining using gratings written in photothermo-refractive (PTR) glass will be discussed. The chapter also demonstrates that binary phase profiles may be encoded into volume Bragg gratings, and that for any probe beam capable of satisfying the Bragg condition of the hologram, this phase profile will be present in the diffracted beam. A multiplexed set of these holographic phase masks (HPMs) can simultaneously combine beams while also performing mode conversion. An approach for making HPMs fully achromatic by combining them with a pair of surface gratings will be outlined.

Keywords: holography, volume Bragg gratings, beam combining, phase plates, photothermo refractive glass, multiplexed volume gratings

1. Volume Bragg gratings

1.1. Description and properties

Volume grating as its name suggest is a grating that occupies the volume of a medium. Typically, for such gratings the term volume Bragg gratings (VBGs) is used in relation to Sir William Bragg who in 1915 used diffraction of light propagating through a crystal to determine the crystal's lattice structure [1]. What he found was that at certain conditions the light is strongly diffracted by the crystal. Such condition is called "resonant condition" or also "Bragg condition." Here is also the place to make the distinction between surface and volume Bragg gratings. If we start with a surface grating and start increasing its thickness at some point the different diffraction orders will reduce to a moment where there will be only one order. This defines the transition to a volume grating behavior [2].

There are two basic types of VBGs which is shown in **Figure 1**. The first one is a transmission Bragg grating (TBG) for which if the incident light satisfies the Bragg condition it is not transmitted but also diffracted. The second type is a reflection Bragg grating (RBG) which behaves like a mirror for incoming light that matches the Bragg condition.

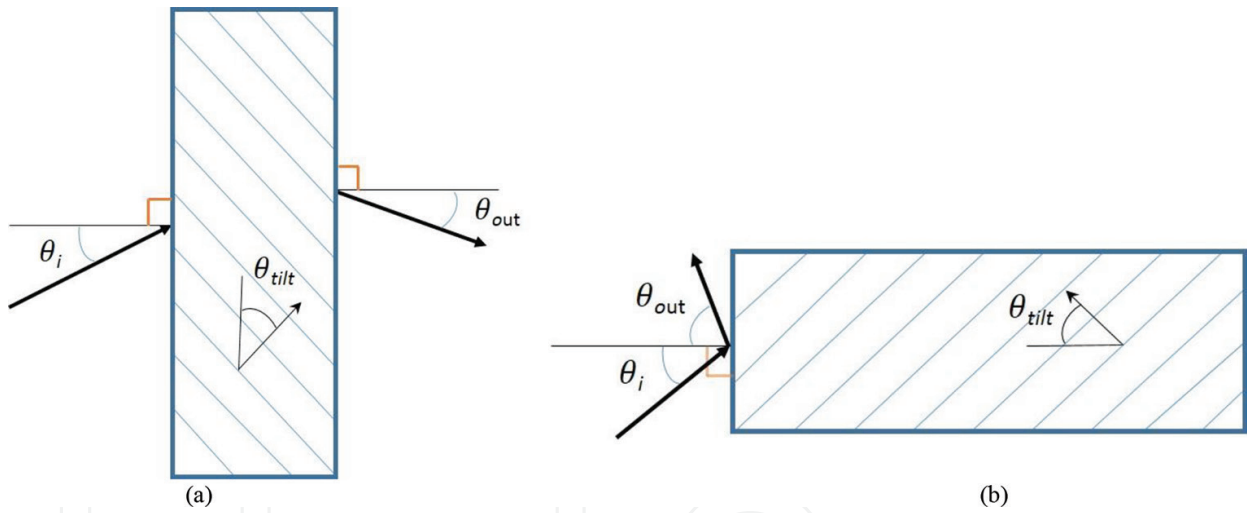


Figure 1. Beam geometries for transmission Bragg grating (a) and for reflective Bragg grating (b).

For simplicity, in **Figure 1**, for both types of volume gratings, the angle of incidence is the same θ_i and the tilt of the volume grating inside the medium is θ_{tilt} . Resonant diffraction from each of these VBGs occurs upon satisfaction of their Bragg conditions which are defined by Eqs. (1) and (2).

$$\lambda_{\text{TBG}} = 2\Lambda \sin(\theta_i + \theta_{\text{tilt}}) \quad (1)$$

$$\lambda_{\text{RBG}} = 2\Lambda \cos(\theta_i + \theta_{\text{tilt}}) \quad (2)$$

Here, Λ is the period of the VBG and λ_{VBG} is the wavelength of the incident light which for the particular θ_i and θ_{tilt} satisfies the Bragg condition. The gratings depicted in **Figure 1** are uniform VBGs that can be recorded in a photosensitive material by simple interference of two

collimated laser beams. The recording wavelength, angle of interference, and the refractive index of the material determine the grating's parameters. There are techniques capable of recording more complex volume gratings which have nonuniform period and for which the Bragg condition will be different depending on the space coordinates [2]. Regardless, if the variation of the period is negligible when compared to the probe beam size used for characterization of the VBG; Eqs. (1) and (2) can still provide the resonance wavelength.

Figure 2 exhibits one example of beam geometry for recording uniform transmitting and reflecting volume gratings. In this recording approach, two plane waves (purple beams) illuminate the sample from one side at a half-angle of interference ϕ . Depending on the direction from which the grating is used, it can either work as a TBG (green beams) or as an RBG (orange beams). Before recording, the grating parameters such as period and modulation need to be calculated so the recording is carried out accordingly.

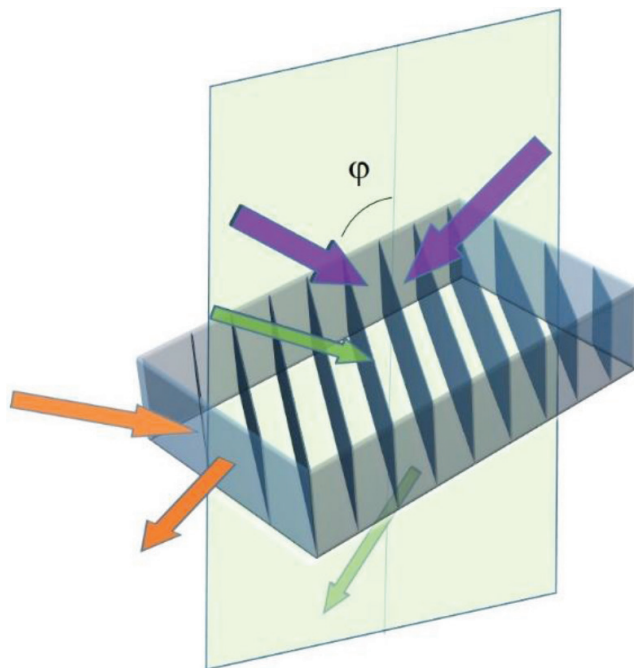


Figure 2. Recording geometry used for recording reflective and transmitting Bragg gratings. The recording beams are shown in purple and the half-angle of interference ϕ determines the properties of the grating. The VBG is utilized as an RBG if probed as the orange beams or as TBG if probed as the green beams.

The main model describing volume Bragg gratings was introduced by Kogelnik [3] in 1969. His model describes that diffraction from a VBG is based on coupled wave theory (CWT) and provides analytical solutions for RBGs and TBGs including tilted ones. **Figures 3(a, b)** and **4(a, b)** present examples of the wavelength and angular responses of an RBG and a TBG correspondingly, calculated using Kogelnik's theoretical approach.

Figures 3 and **4** give good overview of the main properties of TBGs and RBGs. In particular, RBGs are much more suited for implementation as narrow wavelength filters. For example, the full-width half-maximum (FWHM) wavelength selectivity of the reflective grating simu-

lated in **Figure 3(a)** is around 225 pm but it can reach down to 15–20 pm if designed accordingly. TBGs, in contrast, have much wider wavelength acceptance starting at a few hundred picometers and reaching several nanometers. **Figure 4(a)** shows the spectral response of 1.5 mm thick TBG with nodulation of 330 ppm. For these parameters, its FWHM of 2.3 nm is close to an order magnitude larger if compared to the RBG one.

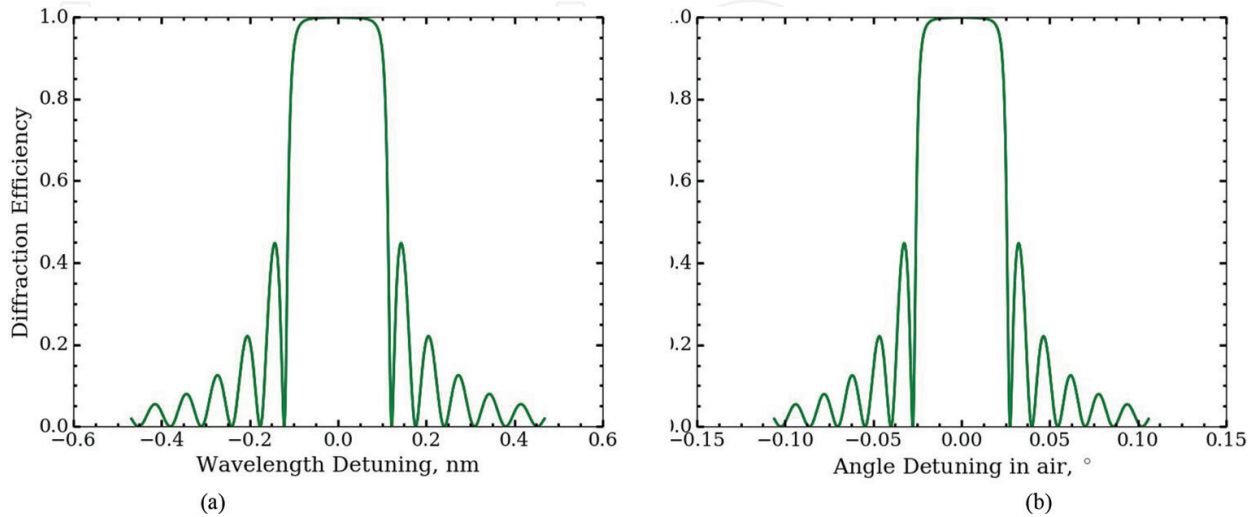


Figure 3. Wavelength (a) and angular (b) response for an RBG. The VBG is 5.5 mm thick, it is 20° tilted, and has a 240 ppm refractive index modulation.

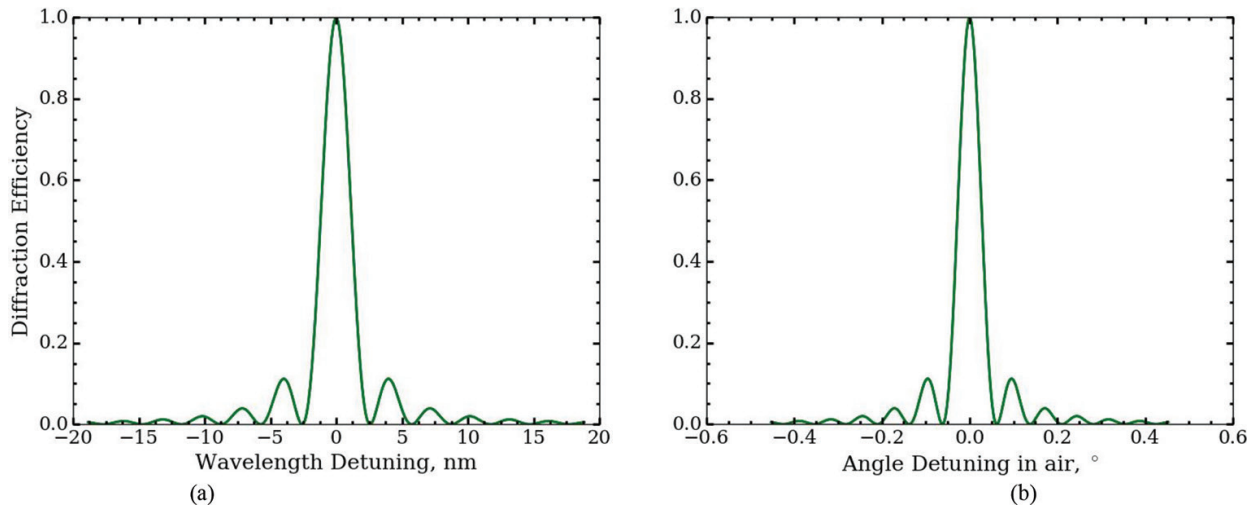


Figure 4. Wavelength (a) and angular (b) response for a TBG. The VBG is 1.5 mm thick, it is 20° tilted, and has a 333 ppm refractive index modulation.

TBGs, alternatively, can be used as narrow angular filters with acceptance values as low as 0.1 mrad, whereas RBGs have typical angular acceptance of more than 10 mrad all the way to 100 mrad. These properties of the two types of VBGs define their use in different applications. For example, the narrow angular selectivity of the TBGs makes them a great angular filter that can be used to suppress higher order modes generation in laser cavities while keeping them very compact [4]. Alternatively, RBGs with their narrow wavelength selectivity can be used

for narrow wavelength beam combining where the diffracted by and the transmitted through an RBG beams can be separated by only a few hundred picometers [5]. Regardless of the close wavelength separation, the RBG does not diffract the transmitted beam even though both beams have a common propagating direction.

Table 1 summarizes the TBG's and RBG's characteristics and their typical range. Until now, we have discussed wavelength and angular selectivity of VBGs but the third very important parameter is the VBG's efficiency. There are two generally accepted ways to define a VBG's efficiency and the more widely used on is the so-called "relative diffraction efficiency." It is defined as normalization of the diffracted to the transmitted by a VBG power. Its advantage is that it removes any losses introduced by the medium. The second way is called "absolute diffraction efficiency," where the diffracted power is normalized to the incident power.

	Transmitting VBG (TBG)	Reflecting VBG (RBG)
Angular selectivity	0.1–10 mrad	10–100 mrad
Spectral selectivity	0.3–20 nm	0.02–2 nm
Diffraction efficiency	Up to 100%	>99.9%

Table 1. TBG and RBG characteristics.

1.2. Recording materials

Recording of a volume grating requires the use of a material that is photosensitive. The modulation of the recording light intensity should create a corresponding refractive index change in the recording material which on a macroscopic level will be in fact the volume Bragg grating. There is a wide variety of photosensitive materials that can be used for recording VBGs [6, 7]. The main requirement that they need to fulfill is to have enough spatial resolution that will allow the recording of gratings with particular periods. The other two factors are the photosensitivity of the material and its dynamic range. The photosensitivity determines the exposure duration and given that VBGs are most commonly recorded by interference of light, it is of great benefit to keep the exposure time as short as possible. The material's dynamic range provides the maximum refractive index change that can be achieved. This property affects the VBGs thickness and the maximum number of volume gratings that can be multiplexed together in the same volume. Other properties that depending on the particular application may be important are the optical damage threshold, the maximum physical dimensions of the material, its losses, its environmental sensitivity, and others.

The most common recording materials are dichromated gelatins, photopolymers, photorefractive crystals, photosensitive fibers, and photothermo refractive glasses. We will not discuss in detail the properties of each of these materials because they have been well investigated in the literature [8–16]. The applications and experimental results shown further in the chapter are based on using photothermo-refractive glass (PTR) due to its capabilities of handling high-power laser radiation because of its low losses, its environmental robustness, and extremely high resolution [14–16].

Photothermo-refractive glass is a relatively new photosensitive material well suited for phase hologram recording. It combines high sensitivity achieved by two-step hologram formation process and high-optical quality resulting from its technological development. The PTR glass is a $\text{Na}_2\text{O-ZnO-Al}_2\text{O}_3\text{-SiO}_2$ glass doped with silver (Ag), cerium (Ce), and fluorine (F). It is transparent from 350 to 2500 nm. The chain of processes, which produce refractive index variation, is as follows: the first step is the exposure of the glass to UV radiation, somewhere in the range from 280 to 350 nm. This exposure results in photoreduction of silver ions Ag^+ to atomic state Ag^0 . This stage is similar to formation of a latent image in a conventional photo film because no significant changes in the optical properties of the glass occur. The final formation of the holographic recording is secured by subjecting the glass to thermal development. During this step, at elevated temperatures, a number of silver containing clusters are formed in the exposed regions of the glass due to the increased mobility of Ag^0 atoms. These silver-containing clusters serve as nucleation centers for the growth of NaF crystals. Interaction of these nanocrystals with the surrounding glass matrix causes the decrease of refractive index. Refractive index change Δn of about 1.5×10^{-3} (1500 ppm) can be achieved and is enough to allow the recoding of high-efficiency hologram into glass wafers with thickness exceeding several hundred microns.

The second consequence of the crystalline phase precipitation in PTR glass is related to its physical properties and is extremely valuable. The NaF crystalline particles in the glass matrix are almost impossible to destroy by any type of radiation which makes PTR holograms stable under exposure to IR, visible, UV, X-ray, and gamma-ray irradiation. For example, laser damage threshold for 8 ns laser pulses at 1064 nm is in the range of 40 J/cm^2 . Also, the non-linear refractive index of PTR glass is the same as that for fused silica which allows the use of PTR diffractive elements in all types of pulsed lasers. Another PTR advantage is its very low losses—on the order of 10^{-5} cm^{-1} . Testing of VBG recorded in the PTR glass performed under irradiation of 9 kW CW with a 6-mm-diameter spot showed heating that did not exceed 15 K [17]. Even though small heating effects lead to thermal variations of the refractive index of the glass ($dn/dt = 5 \times 10^{-8} \text{ K}^{-1}$). In the case of Bragg grating written inside a PTR glass, this feature leads to thermal shift of the Bragg wavelength of around 10 pm/K. It is worth mentioning also that due to the melting temperature of the NaF crystals being almost 1000°C , PTR holograms are stable at elevated temperatures and could tolerate thermal cycling up to 400°C . This temperature is determined by the plasticity point of the glass matrix.

Typically, Bragg gratings in the PTR glass are recorded by an exposure to interference pattern of radiation from a He-Cd laser operating at 325 nm. The spatial frequency of the gratings can vary from 50 up to about $10,000 \text{ mm}^{-1}$, their thickness from 0.5 to 25 mm, and a diffraction efficiency of up to 99.9%.

2. Applications of volume Bragg gratings

2.1. Spectral and coherent laser beam combining by volume Bragg gratings

Single laser sources are limited in terms of maximum power by thermal and nonlinear effects and can achieve no more than few kW. Laser systems that can generate from 10 to 100

kW CW power integrate from several to tens of laser sources. There are several approaches for integrating/combining laser beams but the most common ones are using either volume Bragg gratings, diffractive optical elements, or surface diffraction gratings [18]. This chapter discusses the use of VBGs for laser beam combining including spectral and coherent combining.

Spectral beam combining (SBC) and coherent beam combining (CBC) are two complimentary methods leading toward multi-kilowatt diffraction limited laser sources. In SBC, multiple channels of different wavelengths are superimposed spatially to generate a single output beam. The main advantage of SBC if compared to CBC is the simplified optical setup due to the fact that there is no need to monitor and adjust the phase of the individual beams. The drawback of using SBC is the fact that the spectrum of the combined beam is much broader when compared to the individual input beams. Regardless of this, the final combined output could still have diffraction limited quality. To minimize the wider spectrum issue, it is necessary to use very narrow spectrally selective beam combining elements that will deliver an output beam with minimum spectral bandwidth.

Reflective volume Bragg gratings are holograms that are not angularly dispersive and depending on their design they can be made to be very wavelength selective. Also, they can have diffraction efficiencies close to 100%, and if recorded in a suitable material that can have very low losses, which makes them suitable for high power laser applications. All these facts together make them a very good optical element for implementation in the SBC system. **Figure 5** demonstrates the concept for using a VBG for spectral combining: diffraction efficiency is close to 100% when the Bragg condition is met and is close to 0% at wavelengths shifted away from the Bragg condition and corresponding to the grating's minima in its characteristic curve.

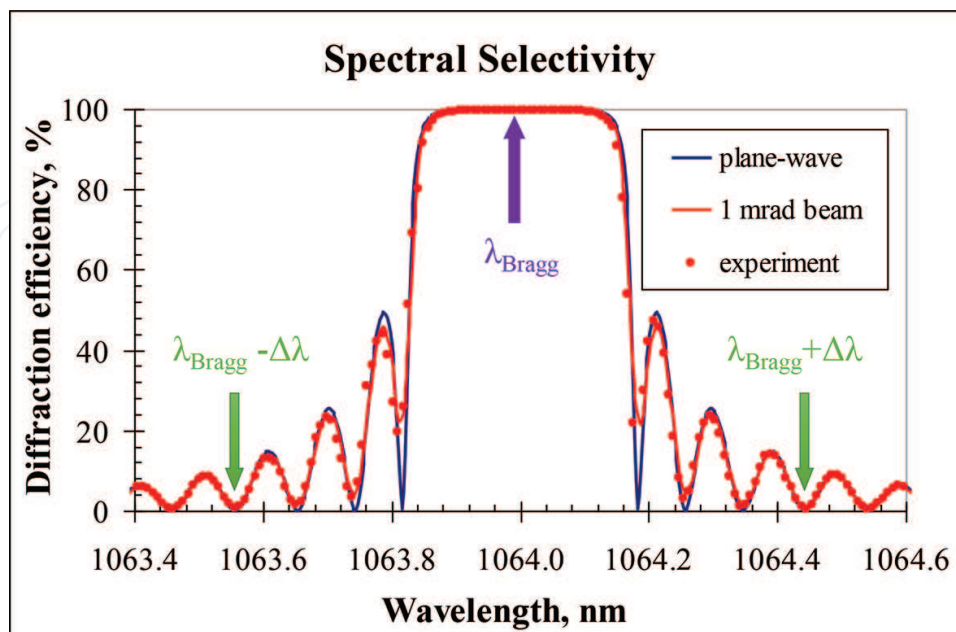


Figure 5. Spectral dependence of the diffraction efficiency of an RBG.

In the example shown in **Figure 6**, two beams with shifted wavelengths are brought to interact with a reflective VBG with characteristic efficiency versus wavelength curve shown in **Figure 5**. This VBG reflects wavelength λ_1 when it satisfies the Bragg condition at a given angle but transmits wavelength λ_2 with minimal losses if it matches with one the VBG's minima (e.g., the fourth one). In this way, the diffracted beam λ_1 and the transmitted beam λ_2 can emerge overlapped and collinear. When using reflective VBGs for spectral beam combining, it is imperative to ensure as high as possible diffraction efficiency for the diffracted beam and minimal diffraction efficiency for the transmitted beam.

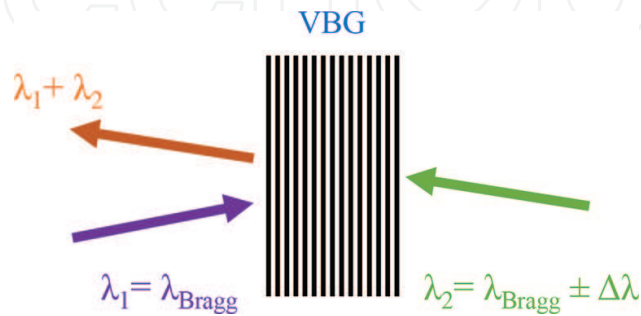


Figure 6. Schematic description of two-beam spectral combining setup using RBG as a combining element.

This approach for SBC can be extended where several VBGs are used to combine more than two laser beams. Such system was presented in [5] and demonstrated the combining of five lasers, each generating 150 W CW to give a total combined power of 750 W (**Figure 7**). Spectrally, the beams were 250 pm apart so the combined spectrum had width of 1 nm in total. For many applications, it is not only the total power that is of significance but also to final beam quality. In this particular example, the M^2 of the combined beam was 1.6 and the beam combining efficiency was greater than 90%. The VBGs were recorded in the PTR glass which, as already mentioned, possesses very low intrinsic losses and therefore can handle high power fluxes with minimal light being absorbed and converted to heat. Regardless, the authors had to implement a thermal tuning and compensation scheme in order to control the resonant conditions of each grating and to manage thermal distortions. As shown in **Figure 7**, the five-beam combining system is quite complex and scaling it to a larger number of channels will scale the mechanical and also thermal management complexity. In addition, the footprint of the systems will also be quite substantial and will make it impractical for use out of laboratory environment.

An approach where a single diffracting optical element that is capable of diffracting several beams simultaneously and substitutes several single beam reflecting elements can reduce the complexity and the space that the beam combining system occupies. Such element can be a computer-generated DOE or one consisting of several mutually aligned VBGs that occupy the same volume. We will discuss in detail the latter where several reflective VBGs are multiplexed such that each laser channel is redirected into a single, common output.

Figure 8 shows the design of a spectral beam combining system capable of combining five laser beams by using a multiplexed VBG (MVBG) element. The MVBG contains four volume Bragg gratings that reflect four beams with different wavelengths correspondingly while

transmitting the fifth beam which is out of resonance with any of the four multiplexed VBGs. This system is fully analogous to the one shown in **Figure 7** but with the benefits of being more compact and simpler to align. The feasibility of the approach was proven and demonstrated in [20] where a double-multiplexed VBG recorded in the PTR glass was used to combine three laser beams. As a first step, the authors combined the two reflected by the MVBG beams to realize a total power of 282 W with combining efficiency of 99%. The M^2 of the combined beam was very close to the lasers' original M^2 of 1.05 and was measured to be 1.15 in the 'X' direction and 1.08 in the 'Y' direction. The MVBG was kept at constant temperature by a placing it in a copper housing in which thermo-electric elements attached to it. This approach allowed keeping the MVBG into resonance with the lasers in the case of heating due to absorption occurred. Heating leads to expansion of the glass and therefore to change of the gratings' periods which, on its own, leads to the lasers falling out of resonance with their corresponding VBGs. At the power density of approximately 3 kW/cm², the authors did not observe any heating problems and therefore no beam quality degradation. Next, the third beam, in this case the transmitted one, was added to the system to achieve a total combined power of 420 W. While the final three beam combining efficiency of 96.5 % was still very high, the total beam quality parameter got worse and reached 1.38 in the 'X' and 1.20 in the 'Y' directions. The worse M^2 was due to heating of the glass introduced by the transmitted beam. Such thermal effect was not observed when combining only reflected beams because they penetrated the MVBG significantly less and therefore much less of their power was absorbed and dissipated as heat into the glass. Using better cooling techniques such as surface air-flow can eliminate the thermal effect and the resulting beam quality degradation observed [17]. In conclusion, the use of multiplexed volume Bragg gratings for spectral beam combining is excellent alternative and addition to the current state of the art combining techniques. The capability of reducing the number of combining elements in the system while being able to manage the thermal load is especially valuable especially when combining kilowatt level laser sources.

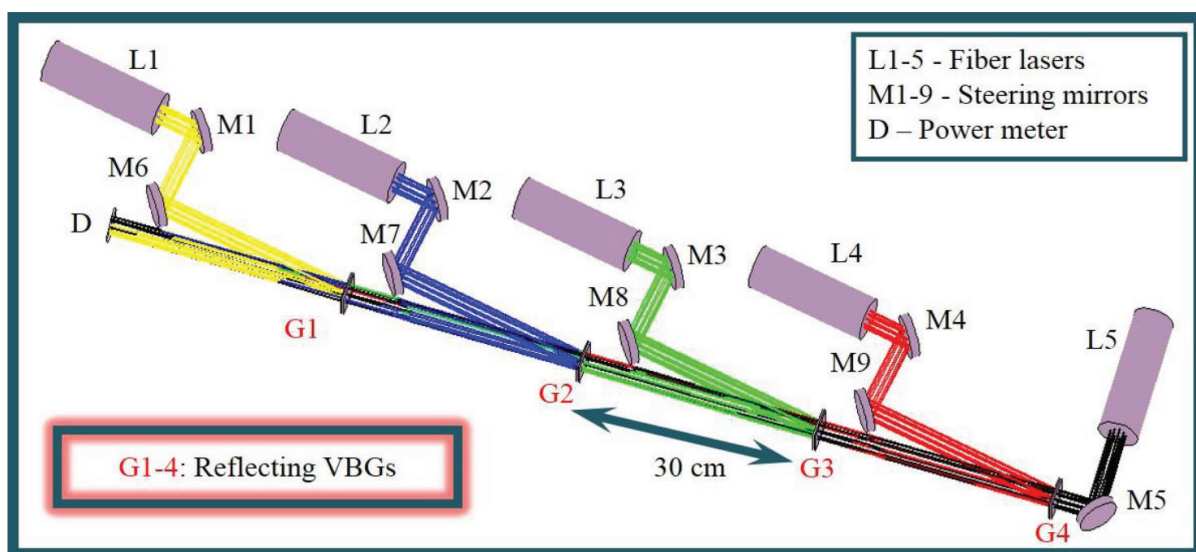


Figure 7. Five -beam combining setup using RBGs as combining elements [32].

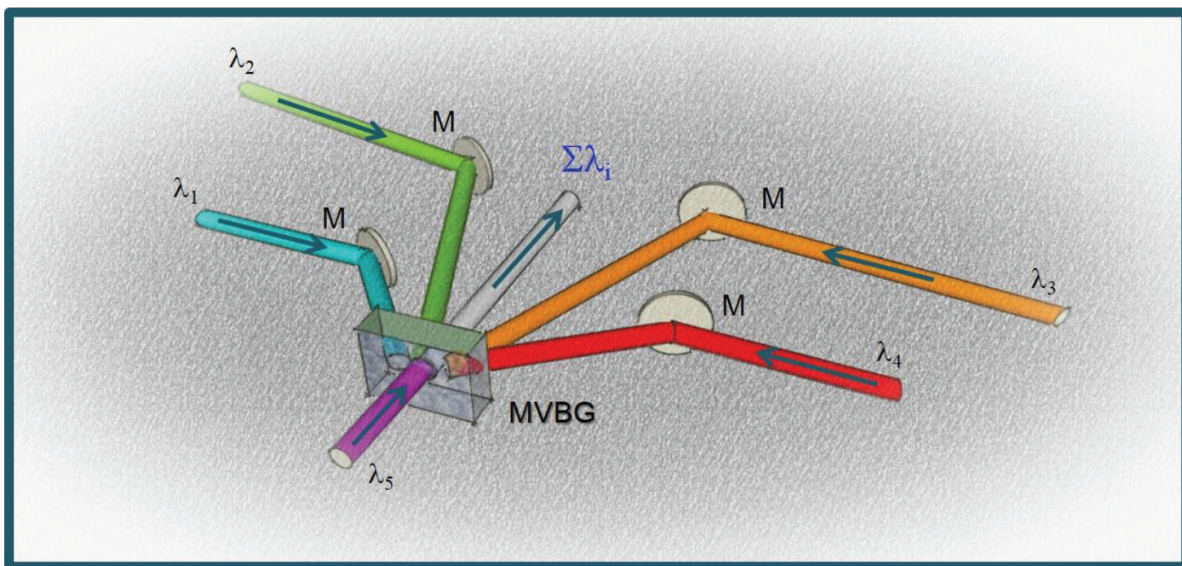


Figure 8. Five-beam combining setup using a single multiplexed VBG as combining element [19].

Volume Bragg gratings can be used for coherent beam combining (CBC) as well [21]. In coherent combining, the lasers are phased to emit coherently at the same wavelength and in phase. Depending on how the phase-locking of the lasers is achieved, CBC can be either passive or active. In the active case, the phase of each of the lasers that are being combined is controlled with high precision using feedback loop. This drastically complicates the whole system from optical and electronics perspective. In the passive approach, the sources share a common resonator and due to this they emit coherently without the need for external phase control. Such system is very simple and compact. Volume Bragg gratings and especially multiplexed ones are the ideal option for use in passive CBC because a system implementing such MVBG will have a single coherently combined output beam. The MVBG is used as 1:N splitter and combiner and it is important that there is equal radiation exchange between each laser.

Such approach was used by [22] where two lasers were coherently combined using a double MVBG. Two identical reflecting VBGs were symmetrically recorded in the PTR glass in such a way that they have a degenerate output. **Figure 9** presents the optical setup of the two-channel system. The output of each of the fiber lasers is reflected in the common/degenerate direction toward the output coupler (OC). The part of the combined output reflected by the OC is split by the MVBG for feedback to the two lasers. Small part of the emission that leaks through the MVBG is used to confirm the mutual coherence of the two lasers by interfering the two lasers. Using this scheme for CBC, the authors reported a combining efficiency of more than 90%, slope efficiency of almost 50%, and fringe contrast of 96%, which indicates a significant degree of coherence between the two channels. A similar scheme can be realized using multiplexed transmitting Bragg grating as well.

The design of the multiplexed VBG is quite important in order for the systems as whole to operate with high combining and slope efficiencies. For example, losses due to lower than 99% diffraction efficiency of the gratings lead to losses in both the combining and the splitting processes in a given resonator round trip.

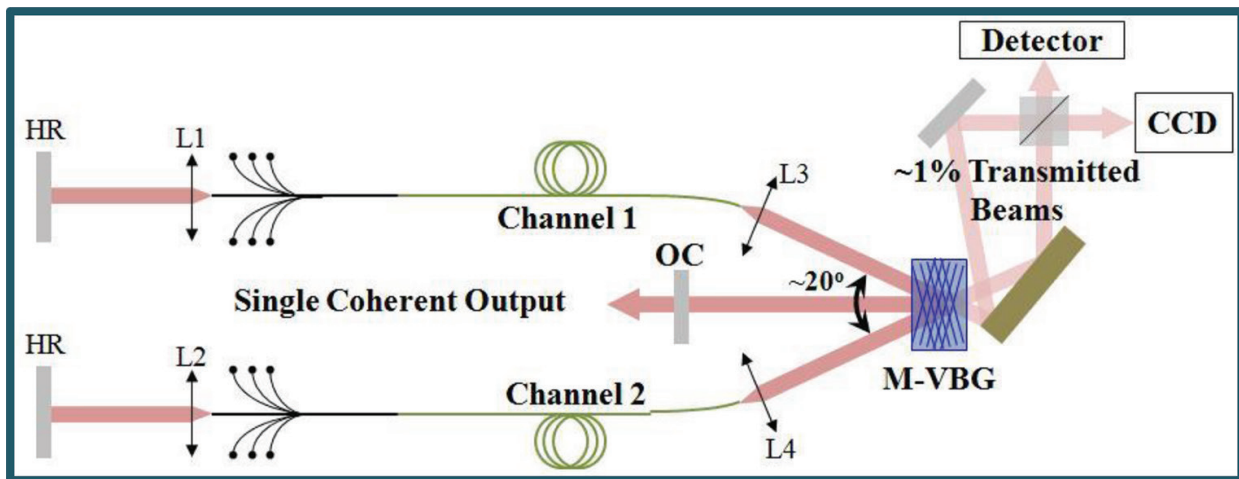


Figure 9. Coherent beam combining setup using double RBG as a combining element [22].

In conclusion, an approach for passive coherent beam combining capable of delivering from kW to tens of kW narrow-linewidth laser power is highly desired and sought after. Passive CBC using multiplexed volume Bragg gratings is a very promising technique that can deliver such power levels with great efficiency and minimal system complexity.

2.2. Holographic phase masks and their applications

Phase masks have found numerous applications in areas such as beam shaping, laser mode conversion, encryption, and others. The two most common ways to make phase masks are either by using a contoured surface where the path length for different parts of the beam is different or by using a bulk material inside which localized refractive index changes are made. In both cases, the phase shift is done by changing the local optical propagation path and therefore the phase masks are limited to use at a specific wavelength. This limits substantially their potential for use in different applications. The solution will be to make an achromatic phase mask and some attempts have been performed in the past [23–25]. For example, multiplexing many computer-generated holograms is one approach where arbitrary wavefronts can be generated if the mask is illuminated with a suitable beam. For this approach to work, a separate hologram needs to be recorded for every desired wavelength which makes the method quite complicated. A simpler and more flexible approach for making achromatic phase masks will be described in this section of the chapter.

The foundation of the approach is to encode phase mask profile into transmitting Bragg grating, which as whole works as a so-called “holographic phase mask” (HPM). This HPM can be implemented for a broad range of wavelengths and for each one of them it produces the desired diffracted phase profile, as long as the Bragg condition of the TBG is met for the given wavelength. As it will be shown, such HPM can be made fully achromatic by introducing two surface diffraction gratings with particular periods, before and after the HPM. In this way, no angular Bragg angle tuning is required. As expected, HPMs utilize the diffraction properties of regular TBGs and therefore they can diffract up to 100% of a beam into a single order.

Another specific property of TBGs is that they have relatively narrow angular selectivity and that allows the multiplexing several HPMs into one piece of recording materials, while having little or no cross-talk between them.

To help understand the way HPMs work, it is important to note that a volume Bragg grating is the simplest volume hologram that can diffract different wavelengths without distorting the initial beam profile (as long as they satisfy the Bragg condition) which sets it apart from more complex holograms, which are capable of changing the beam wavefront. Also, this leads to the fact that HPM can be tested with wavelength different or the same as the recording one.

The encoding of a phase profile into a TBG can be carried out by using a holographic setup shown in **Figure 10** [26]. In the setup, a standard binary phase mask (see **Figure 11**) is placed into one of the arms (object beam) of a two-beam-recording system. It is important to emphasize that the phase mask must have the desired phase transitions for the hologram recording wavelength and not for the reconstructing wavelength. The beams interfere at an angle θ relative to the normal of the sample to create a fringe pattern inside the sample following the equation:

$$I = I_1 + I_2 + 2\sqrt{I_1 I_2} \cos((\vec{k}_1 - \vec{k}_2) \cdot \vec{r} + \phi(x, y, z)), \quad (3)$$

where I is the intensity, \vec{k}_i is the wavevector for each beam, and ϕ is the phase change introduced by the phase mask after the object beam has propagated to the recording material. As described in [26], the recorded hologram will have a refractive index profile described by:

$$n(x, y, z) = n_0 + n_1 \cos(\vec{K} \cdot \vec{r} + \phi(x, y)), \quad (4)$$

where n_0 is the background refractive index, n_1 is the refractive index modulation, and $\vec{K} = \vec{k}_1 - \vec{k}_2$ is the grating vector.

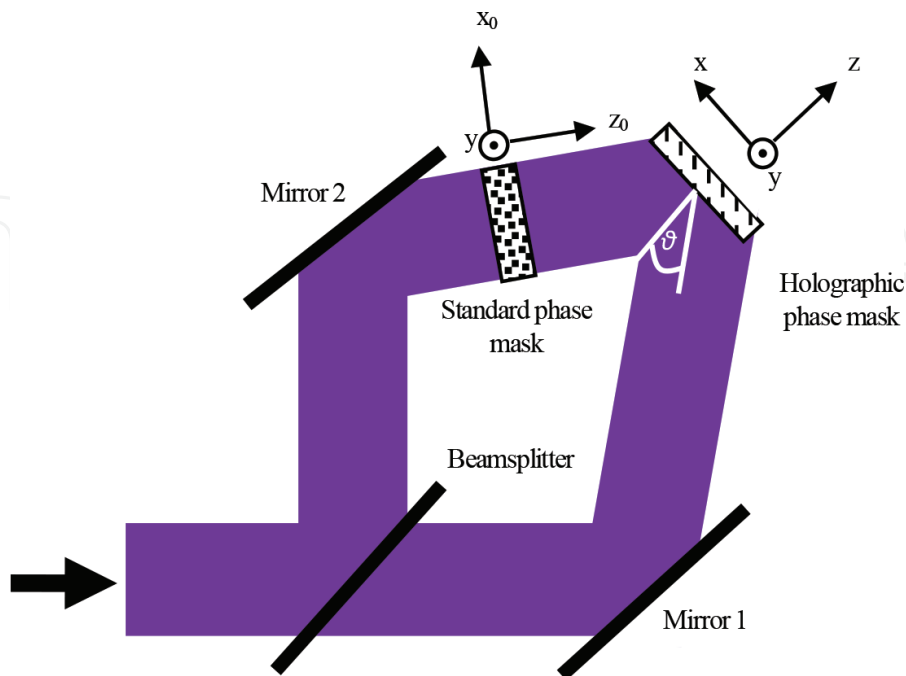


Figure 10. Recording setup used for encoding phase profile into a TBG [26].

By applying coupled wave theory, one can determine the diffracted beam phase profile and diffraction efficiency of a beam satisfying the Bragg condition of an HPM [3]. The model was applied for the binary phase profile encoded in a TBG as the one shown in **Figure 11**.

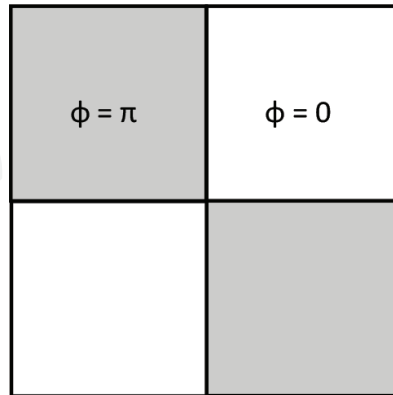


Figure 11. Binary phase distribution for a four-sector phase mask.

Applying binary π phase shift to a regular TBG along both the x - and the y -axis will determine if there are any orientation-dependent variations in the output beam's phase profile or diffraction efficiency. The performance of the HPM was simulated for 632 and 975 nm. The parameters of the TBG were the same for both wavelengths just the incident angle was adjusted in order to match the corresponding Bragg condition.

As shown in **Figure 12(b)**, the diffraction efficiency of an HPM can reach the one of a uniform TBG illuminated with a plane wave. The observed lower efficiency for smaller probe beam sizes is due to the fact that the parts of the beam that cross the phase discontinuity will not satisfy the Bragg condition and this affects smaller beams more when their area is comparable to the phase discontinuity total area. For larger beams, this effect is negligible and its influence on the diffraction efficiency is very little. **Figure 12(c)** shows that the π phase shift is present for all three wavelengths when it is along the x -axis. The slight offset of the phase shift from the origin is due to the propagation of the test beam through the HPM and the diffraction that occurs only in the x -direction. In the case when the phase jump is along the y -axis, as shown in **Figure 12(d)**, it is as well present for all wavelengths but the discontinuity is centered exactly at the origin because the test beam does not have a component propagating in the y -direction. In conclusion, HPMs have the wavelength and angular diffraction properties of regular TBGs, while capable of encoding a desired phase profile on to a test beam over its whole bandwidth as long as it satisfies the Bragg condition.

Experimentally, HPMs were fabricated and characterized using PTR glass and some of the results will be discussed here [27]. As a master phase mask was used a four-sector one, as shown in **Figure 11**. The mask was designed to give π phase shift for the hologram recording wavelength of 325 nm. For comparison purposes, a regular TBG was also recorded in the same piece of PTR glass by removing the phase mask and rotating the sample. Such multiplication guarantees that both diffractive elements share the same glass volume and therefore any localized glass inhomogeneity will influence both of them in the same way. **Figure 13** shows the measured diffraction efficiencies of the HPM and the standard TBG. The results match very

well the theoretically predicted small difference in efficiency due to the phase shift areas and also show that HPMs behave as regular TBGs in terms of angular selectivity properties.

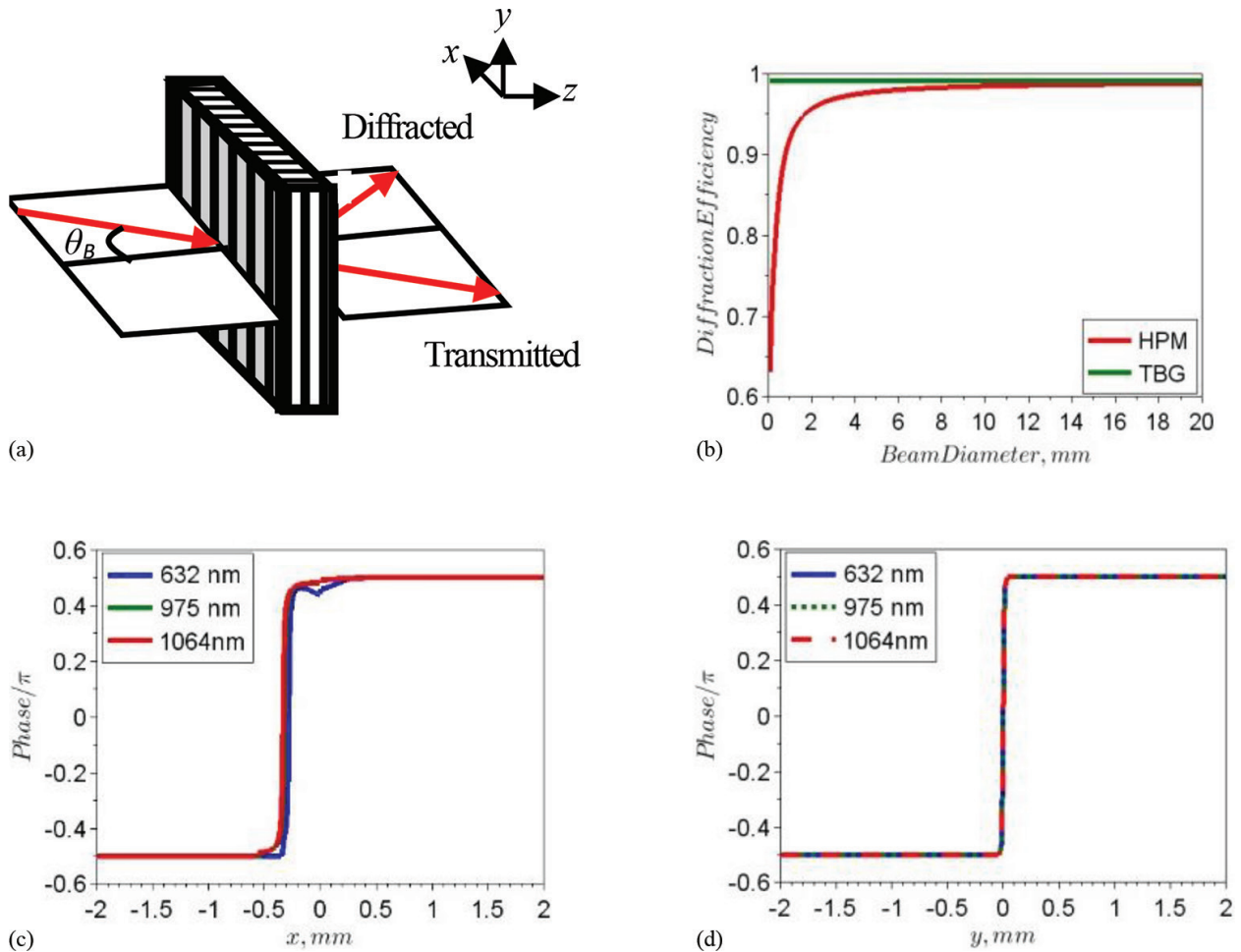


Figure 12. (a) Schematic representation of beam incident on HPM, (b) diffraction efficiency of an HPM at 1064 nm as a function of beam diameter when a binary phase dislocation is encoded along the x -axis, (c) the diffracted beam phase profile when a binary phase dislocation is encoded along the x -axis for beams of different wavelength, (d) the diffracted beam phase profile when a binary phase dislocation is encoded along the y -axis for beams of different wavelength.

HPM, as the one just theoretically discussed, was experimentally realized and used to demonstrate its capabilities as an optical mode converter that can operate at different wavelengths. To show the unique properties of HPMs, the fabricated element was tested with three different wavelengths (632.8, 975, and 1064 nm). A standard binary four-sector phase mask can convert a Gaussian beam to a TEM_{11} mode if properly aligned to the center of the phase jump boundaries. **Figure 14** demonstrates the far-field intensity pattern for a simulated mode conversion through a binary phase mask (a) and the patterns experimentally observed for three different wavelengths after diffraction by the HPM (b–d). The diffracted beam profiles clearly exhibit the four-lobed pattern which confirms the notion that the phase profile imprinted in the HPM is present in the diffracted beam and this fact applies for very broad range of wavelengths. Unlike standard phase masks which can only operate for one predetermined wavelength for which the corresponding phase shift is as required. This example demonstrates the

great potential that HPMs possess given that laser and fiber modes are present in almost any optical system and their conversion to other modes is of great interest.

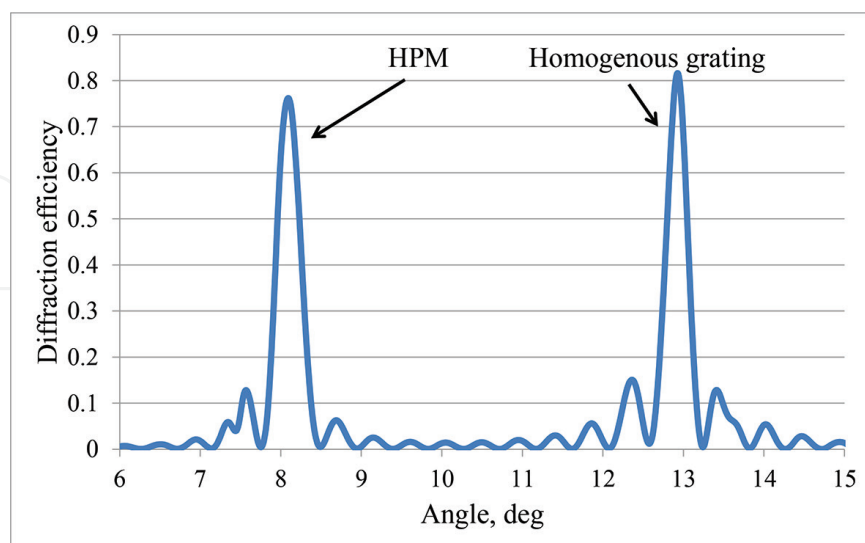


Figure 13. Diffraction efficiency angular spectrum of an HPM and homogenous grating.

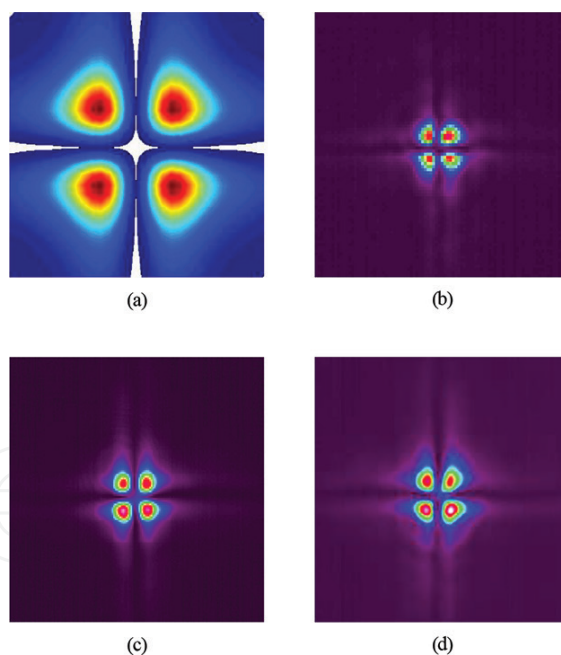


Figure 14. (a) Simulated far-field profile of a beam after passing through an ideal four-sector binary mask and the diffracted beam from a four-sector HPM at (b) 632.8 nm, (c) 975 nm, and (d) 1064 nm. The sizes shown here are not to scale [27].

We already described that multiplexing of volume Bragg gratings can be used for laser beam combining. The same approach can be applied to HPMs and as a result fabricate an element with unique functionality. The property of the HPMs to do mode conversion is not unique [28, 29], but if this is integrated with the capability of VBGs to do beam combining, an element

will be created that can simultaneously convert multiple beams into different modes while combining them to a single beam. For example, fiber lasers that operate at higher order mode are of interest because they are considered to overcome the power limitations of fiber lasers operating at the fundamental mode. Therefore, beam combining several lasers operating at higher order modes into one high-power fundamental mode beam will be very beneficial and of interest as a power scaling approach.

As an example, **Figure 15** shows how a double multiplexed HPM can convert individually two TEM_{11} modes (**Figure 15a** and **15b**) to TEM_{00} modes (**Figure 15c** and **15d**) while also spectrally beam combining the beams into one beam (**Figure 15e**) [27]. The lasers were operating at 1061 and 1064 nm and the HPM consisted two four-sector phase masks integrated in two TBGs that had a generate output. The authors attributed the difference between the far-field profiles of the two laser beams after their conversion to different collimations. In the final combined beam, there are wings present but these were credited to the generation of the initial TEM_{11} modes which was done by a set of HPMs. This brought some alignment challenges as shown in **Figure 15(c)** and. Nevertheless, it is evident that the integration of VBGs and phase plates could open new optical design spaces in areas such as high-power beam combining, mode multiplexing in communication systems, and others.

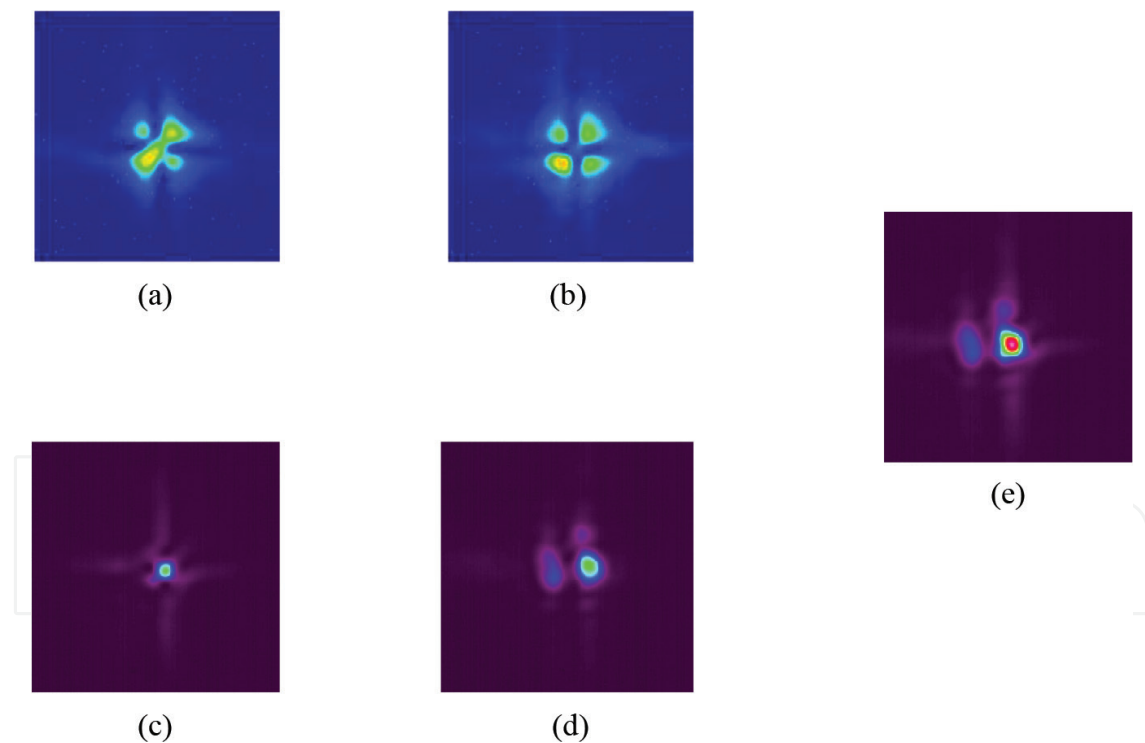


Figure 15. Demonstration of conversion from the TEM_{11} mode to TEM_{00} for 1061 and 1064 nm lasers separately (a, c and b, d); a multiplexed four-sector HPM spectrally combines the two beams and converts them to TEM_{00} (e).

3. Achromatization of HPM with surface diffraction gratings

As discussed, HPMS can successfully imprint their phase pattern as long as the wavelength satisfies the Bragg condition but to achieve this, the HPM needs to be angle tuned which can-

not be considered pure achromatization. Such achromatization of HPMs can be accomplished with the concept of pairing the Bragg grating with two surface gratings [30]. According to the grating dispersion equation (Eq. (5)), a surface grating with a given period (Λ_{SG}) will diffract normally incident light at an angle (θ) as a function of its wavelength (λ):

$$\Lambda_{SG} \sin \theta = m\lambda \quad (5)$$

Based on coupled wave theory [2], a VBG will diffract light if the Bragg condition (Eq. (6)) is met and can reach diffraction efficiencies as high as $\approx 100\%$ [3]:

$$2\Lambda_{VBG} \sin \theta_B = \lambda \quad (6)$$

Since both of these diffraction angles are dependent on the corresponding grating periods, if the surface grating period is double the period of the volume Bragg grating (Eq. (7)), then any first-order diffraction by normally incident light will be at the corresponding Bragg condition of the volume Bragg grating and that will hold for any wavelength [30]:

$$2\Lambda_{VBG} = \Lambda_{SG} \quad (7)$$

Therefore, a surface grating with twice the period of a TBG can make different wavelengths get diffracted by the TBG at the same time as long as they have the same incident angle. In order to recollimate the diffracted beams, an identical surface grating needs to be added in a mirror orientation to the transmitting volume Bragg grating, as shown in **Figure 16**. This grating completely cancels out the dispersion of the first surface grating and recollimates the outgoing beam. Applying this concept to an HPM will eliminate the need for angle tuning in order to meet the Bragg condition for different wavelengths, making, therefore, the device a fully achromatic phase element.

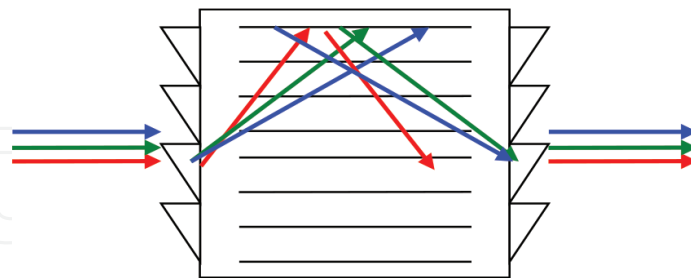


Figure 16. Concept of using surface grating pairs to meet the Bragg condition for various wavelengths regardless of angle tuning [30].

The experimental proof was carried out by using two surface gratings with a groove spacing of 150 lines/mm (a period of $6.66 \mu\text{m}$) aligned to an HPM with a period of $3.4 \mu\text{m}$ in setup shown in **Figure 17** [31]. The goal of the experiment was to achieve successful broadband mode conversion from a Gaussian to a TEM_{11} mode without the need to angularly tune the HPM. Three different TEM_{00} tunable diode laser sources were used in order to get a wavelength range of over 300 nm (765–1071 nm).

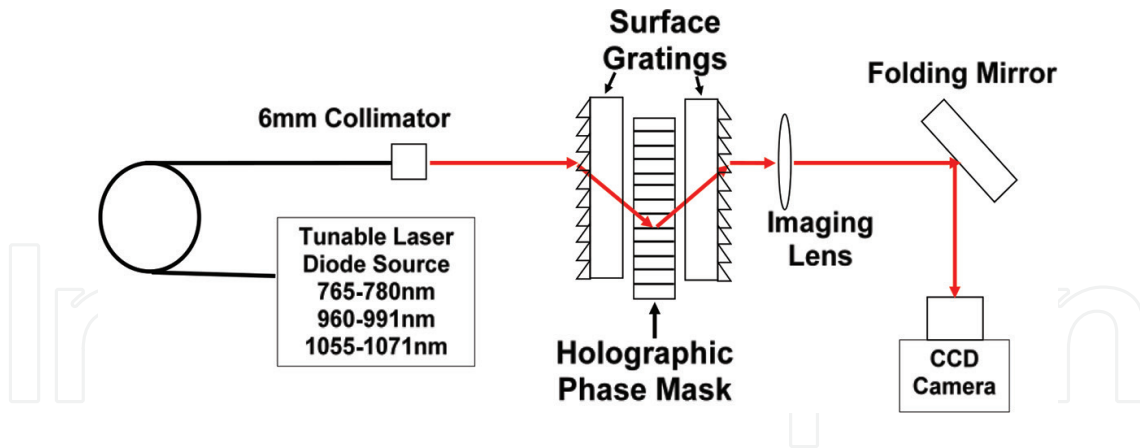


Figure 17. Experimental setup for observing Gaussian to TEM_{11} conversion of the HPM surface grating system with three different diode sources [31].

Figure 18 shows as an example, the far-field profiles of three different wavelengths ((a) 765, (b) 978, and (c) 1071 nm) that were converted to the TEM_{11} mode without any angular adjustment of the HPM. This successfully demonstrates that full achromatization of a holographic phase mask can be achieved with the combination of surface gratings and phase-encoded transmitting volume Bragg grating.

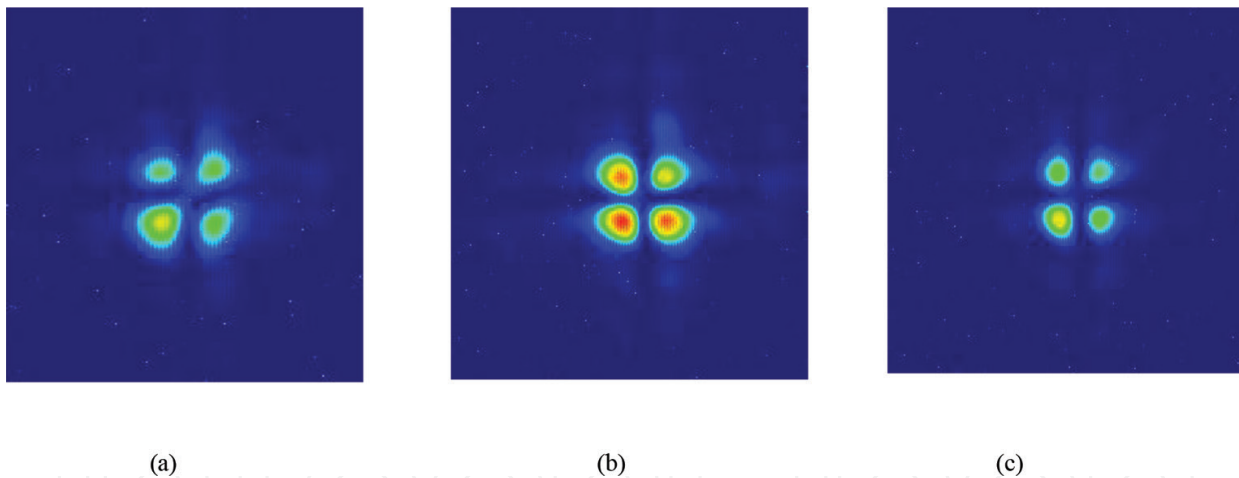


Figure 18. Far-field profile of the diffracted beam after propagating through a holographic four-sector mode converting mask aligned to two surface gratings at (a) 765 nm, (b) 978 nm, and (c) 1071 nm. The sizes shown are not to scale.

In conclusion, this is a demonstration of a way to make phase masks fully achromatic—something not possible until recently. This is achieved by the combination of surface gratings and phase-encoded transmitting volume Bragg grating.

4. Conclusion

The chapter discussed the nature and properties of volume Bragg gratings and presented several of the broad number of applications where VBGs find use. The opportunities to multiplex

VBGs and integrate them with specific phase profiles were shown to bring unique capabilities that are hard or impossible to achieve by other means. VBGs are and will continue to benefit the development and the abilities of many laser and optical systems.

Author details

Ivan Divliansky

Address all correspondence to: ibd1@creol.ucf.edu

The College of Optics & Photonics (CREOL), University of Central Florida, Orlando, FL, USA

References

- [1] W. H. Bragg and W. L. Bragg, *X Rays and Crystal Structure*. London: G Bell and Sons, Ltd., 1915.
- [2] R. R. Syms, *Practical Volume Holography*. Oxford, UK: Clarendon Press, pp. 48, 64, 132–162, 1990.
- [3] H. Kogelnik, “Coupled Wave Theory for Thick Hologram Grating,” *Bell Syst. Tech. J.*, vol. 48, no. 9, pp. 2909–2945, 1969.
- [4] B. M. Anderson, G. Venus, D. Ott, E. Hale, I. Divliansky, D. R. Drachenberg, J. Dawson, M. J. Messerly, P. H. Pax, J. B. Tassano, and L. B. Glebov, “Higher order mode selection for power scaling in laser resonators using transmitting Bragg gratings”, Proc. SPIE 9466, Laser Technology for Defense and Security XI, 94660C, 2015.
- [5] D. Drachenberg, I. Divliansky, G. Venus, V. Smirnov, and L. Glebov, “High-power spectral beam combining of fiber lasers with ultra high-spectral density by thermal tuning of volume Bragg gratings”, SPIE Photonics West 2011, Proc. SPIE 7914, 79141F, 2011.
- [6] L. H. Lin, “Method of Characterizing Hologram-Recording Materials,” *J. Opt. Soc. Am.*, vol. 61, no. 2, pp. 203–208, 1971.
- [7] R. Collier, C. Burchardt, and L. Lin, *Optical Holography*. New York: Academic, 1971.
- [8] B. J. Chang and C. D. Leonard, “Dichromated gelatin for the fabrication of holographic optical elements,” *Appl. Opt.*, vol. 18, no. 14, pp. 2407–17, 1979.
- [9] W. S. Colburn and K. A. Haines, “Volume hologram formation in photopolymer materials,” *Appl. Opt.*, vol. 10, no. 7, pp. 1636–41, 1971.
- [10] S.-D. Wu and E. N. Glytsis, “Holographic grating formation in photopolymers: analysis and experimental results based on a nonlocal diffusion model and rigorous coupled-wave analysis,” *J. Opt. Soc. Am. B*, vol. 20, no. 6, p. 1177, 2003.

- [11] F. S. Chen, J. T. LaMacchia, and D. B. Fraser, "Holographic Storage in Lithium Niobate," *Appl. Phys. Lett.*, vol. 13, no. 7, pp. 223, 1968.
- [12] S. I. Stepanov, "Applications of photorefractive crystals," *Rep. Prog. Phys.*, vol. 57, pp. 39–116, 1994.
- [13] S. Dewra, V. Grover, and A. Grover, "Fabrication and applications of fiber bragg grating—a review," *Adv. Eng. Tec. Appl.*, vol. 4, no. 2, pp. 15–25, 2015.
- [14] L. B. Glebov, "Kinetics modeling in photosensitive glass," *Opt. Mater. (Amst)*, vol. 25, no. 4, pp. 413–418, 2004.
- [15] O. M. Efimov, L. B. Glebov, and V. I. Smirnov, "High-frequency Bragg gratings in a photothermorefractive glass," *Opt. Lett.*, vol. 25, no. 23, pp. 1693–5, 2000.
- [16] O. M. Efimov, L. B. Glebov, and V. I. Smirnov, "Diffractive optical elements in photosensitive inorganic glasses," *Inorg. Opt. Mater.*, vol. 4452, pp. 39–47, 2001.
- [17] B. Anderson, S. Kaim, G. Venus, J. Lumeau, V. Smirnov, B. Zeldovich, and L. Glebov, "Forced air cooling of volume Bragg gratings for spectral beam combination," *Proc. SPIE. 8601, Fiber Lasers X: Technology, Systems, and Applications, 86013D*. (March 22, 2013) doi: 10.1117/12.2005951.
- [18] T. Y. Fan, "Laser beam combining for high-power, high-radiance sources," *IEEE J. Sel. Top. Quantum Electron.*, vol. 11, no. 3, pp. 567–577, 2005.
- [19] I. Divliansky, D. Ott, B. Anderson, D. Drachenberg, V. Rotar, G. Venus, and L. Glebov, "Multiplexed volume Bragg gratings for spectral beam combining of high power fiber lasers", *SPIE Photonics West 2012, Proc. SPIE 8237, 823705*, 2012.
- [20] D. Ott, I. Divliansky, B. Anderson, G. Venus, and L. Glebov, "Scaling the spectral beam combining channels in a multiplexed volume Bragg grating", *Opt. Express*, vol. 21, no. 24, pp. 29620, 2013.
- [21] A. Jain, D. Drachenberg, O. Andrusyak, G. Venus, V. Smirnov, and L. Glebov, "Coherent and spectral beam combining of fiber lasers using volume Bragg gratings," *Proc. SPIE*, vol. 7686, p. 768615, 2010.
- [22] A. Jain, O. Andrusyak, G. Venus, V. Smirnov, and L. Glebov, "Passive coherent locking of fiber lasers using volume Bragg gratings," *Proc. SPIE 7580*, 2010, vol. 7580, p. 75801S.
- [23] D. Mawet, C. Lenaerts, V. Moreau, Y. Renotte, D. Rouan and J. Surdej, "Achromatic four quadrant phase mask coronagraph using the dispersion of form birefringence," in *Astronomy with High Contrast Imaging*, C. Aime and R. Soummer, ed., *EAS Publications Series*, vol. 8, pp. 117–128, 2003.
- [24] J. Rosen, M. Segev, and A. Yariv, "Wavelength-multiplexed computer-generated volume holography," *Opt. Lett.* Vol. 18, no. 9, pp. 744–746, 1993.
- [25] T. D. Gerke and R. Piestun, "Aperiodic volume optics," *Nat. Phot.* vol. 4, pp. 188–193, 2010.

- [26] M. SeGall, I. Divliansky, C. Jollivet, A. Schülzgen, and L.B. Glebov, "Holographically encoded volume phase masks", *Optical Engineering*, vol. 54, no. 7, pp. 076104–076104, 2015.
- [27] M. SeGall, I. Divliansky, C. Jollivet, A. Schulzgen, and L. Glebov, "Simultaneous laser beam combining and mode conversion using multiplexed volume phase elements," *SPIE LASE, Photonics West*, 89601F-89601F-6, 2014.
- [28] A. Shyouji, K. Kurihara, A. Otomo, and S. Saito, "Diffraction-grating-type phase converters for conversion of Hermite-Laguerre-Gaussian mode into Gaussian mode," *Appl. Opt.* vol. 49, no. 9, pp. 1513–1517, 2010.
- [29] M. Beresna, M. Gecevičius, P. G. Kazansky, and T. Gertus, "Radially polarized optical vortex converter created by femtosecond laser nanostructuring of glass," *Appl. Phys. Lett.* vol. 98, pp. 201101, 2011.
- [30] L. Glebov, V. Smirnov, N. Tabirian and B. Zeldovich, "Implementation of 3D angular selective achromatic diffraction optical grating device", *Frontiers in Optics 2003*, Talk WW3.
- [31] I. Divliansky, E. Hale, M. SeGall, D. Ott, B. Y. Zeldovich, B. E. A. Saleh, and L. B. Glebov, "Achromatic phase elements based on a combination of surface and volume diffractive gratings", *Proc. SPIE 9346, Photonics West: Components and Packaging for Laser Systems*, 93460Q, 2015.
- [32] I. Divliansky, A. Jain, D. Drachenberg, A. Podvyaznyy, V. Smirnov, G. Venus, L. Glebov, "Volume Bragg lasers," *Proc. SPIE 7751, XVIII International Symposium on Gas Flow, Chemical Lasers, and High-Power Lasers*, 77510Z, 2010.

